IEEE Access
Multidisciplinary | Rapid Review | Open Access Journal

Received 13 December 2022, accepted 21 December 2022, date of publication 26 December 2022,
date of current version 5 January 2023.

Digital Object Identifier 10.1109/ACCESS.2022.3232403

RESEARCH ARTICLE

Understanding the Electro-Rheological Aspects of Nano Silica Based Ester Fluid With Surfactants and Deep Learning-Based Prediction of ECT

S. K. AMIZHTAN[1], (Graduate Student Member, IEEE), R. AKASH[1], RAMESH L. GARDAS[2], R. SARATHI[1], (Senior Member, IEEE), AND B. ARYANANDINY[3]

[1]Department of Electrical Engineering, IIT Madras, Chennai 600036, India
[2]Department of Chemistry, IIT Madras, Chennai 600036, India
[3]Department of Electrical Engineering, Rajiv Gandhi Institute of Technology, APJ Abdul Kalam Technological University, Thiruvananthapuram 695016, India

Corresponding author: B. Aryanandiny (nandiny.arya@rit.ac.in)

ABSTRACT The present study deals with understanding the impact of different surfactants with nano-silica based ester fluid on its electrical and rheological properties. The stability of nanofluid is of prime concerns, which is achieved by the inclusion of ionic and non-ionic surfactants viz. cetyl trimethyl ammonium bromide (CTAB), oleic acid and Span-80. It is observed that CTAB as surfactant has shown discharge resistance property along with high breakdown strength enhancement of up to 39.5% with ester nanofluid. It is observed that fluorescent fiber technique is more sensitive to identify the inception of corona discharge as compared to Ultra high frequency sensor. The permittivity and tan δ of the fluid have shown marginal increase with the addition of surfactants, irrespective of temperature of the fluid. Rheological properties of the liquid showed only Newtonian flow behaviour even upon inclusion of the surfactant. The viscosity of the base fluid and the nanofluids exhibits similar decay rate at higher temperatures. Electrostatic charging tendency (ECT) derives the correlation between rotation speed and the static current measured adopting spinning disc technique. In addition, the performance of Long Short-Term Memory (LSTM) model is efficient compared to Artificial Neural Network (ANN) model adopted in predicting the charging tendency incorporating electro-rheological parameters at distinct temperatures. The electrical and rheological characteristics suggests the implication of nanofluids with surfactant to enhance the insulation performance for transformer applications.

INDEX TERMS ANN, corona, ECT, ester fluid, LSTM, nanofluids, newtonian.

I. INTRODUCTION

Transformers forms an important component in the power system network and its life relies on proper insulation design. Recently, natural ester-based fluids are gaining importance to use as insulant in transformers because of its better dielectric performance, high fire point and are bio degradable [1], [2].

The world over researchers have indicated that addition of nanofillers to the fluid can enhance the electrical, thermal and rheological properties of the fluid, to use as insulant in transformers. Conventionally, conducting particles, oxides, and nitride particles are used as nanofillers, improving the dielectric performance of the liquid. Miao et al. studied the impact of nanoparticles on the polarization capability of the fluid comparing experimental and modelled parameters [3]. Suspended nanoparticles in liquid act as electron scavengers, converting high-mobility electrons to slow negatively charged particles, preventing the initiation and migration of streamers, and improving breakdown strength [4].

Nano Silica is used as filler material, which showed high dielectric strength and thermal conductivity. Chemically altering the fluid, changing the pH [5] and addition of surfactant [6] are some of the proven techniques to make the insulation fluid more stable. To enhance the stability of nanoparticles in ester fluids, surfactants with ionic and non-ionic structures, such as cetyl trimethyl ammonium bromide

The associate editor coordinating the review of this manuscript and approving it for publication was Kathiravan Srinivasan.

(CTAB), oleic acid and Span-80 are used this study. CTAB are cationic surfactant carrying a positive charged head and oleic acid are anionic in nature with a negative charged head. Span 80 are non-ionic surfactants with lipophilic head and are charge less.

Incipient discharges that occur in transformer insulation can lead to catastrophic failure of the insulation system. There are multiple techniques present to identify the discharges, including electrical, acoustic, ultra-high frequency (UHF) sensors, optical techniques, dissolved gas analysis (DGA), etc. It was recently identified that UHF and fluorescent fiber technique could identify incipient discharges as a condition monitoring tools in transformers.

In power transformers, one of the major issues is the formation of static charges by the circulation of oil, which accumulates surface charges and raises their potential on pressboard materials. Various techniques were adopted to understand the static charge formation, viz., the mini static charge tester, drainage valve measuring, duct oil flow models, spinning disc systems, ECT probe techniques, etc. [7]. Spinning disc is a simple technique to govern the centrifugal forces with the formation of electrical double layer at fluid/pressed board interfaces. It is essential to understand the fluid flow behaviour of the ester-based fluids. Viscosity, conductivity, and shear rate affect drive current production [8]. The generation of flow currents in which the viscoelastic properties of the fluid change due to shear stresses and deformations, exhibiting a rheological pattern of insulating fluids. The study on static charge formation due to nanofluids is highly limited in literature to understand the phenomenon of nanofluidic flow at the pressure plate interfaces.

Considerable work has been carried in the literature using machine learning strategies for various transformer related applications. Majidi et al proposed an ANN based technique to recognize the pattern of partial discharge signals, based on the extracted features the discharge signals were classified [9]. Different models is adopted for the short term electricity load forcasting with CNN, LSTM and ANN [10]. Recently, long short-term memory (LSTM) is gaining importance and proven to be more reliable to predict any defect and performance evaluation. Amir et al correlated the experimental data and literature database for nanofluids to predict the viscosity and ANN modelling to estimate the developed correlation [11]. Kong et al. proposed a recurrent neural network (RNN) based LSTM model for short term load forecasting for an individual electric consumer using a real time data [12]. Shang et al estimated the loss of life (LOL) of the transformer by considering load trends and temperature as inputs by using a stacked LSTM. The LSTM model was trained to capture the load trends and their correlation simultaneously to estimate the LOL [13].

Having known all these aspects, the following important studies were carried out: (a) Identification of a suitable surfactant to achieve uniform dispersion of nano silica in ester fluid and characterization through zeta potential measurement and particle measurement studies. (b) Variation in corona discharge voltage inception in nano ester fluid identified through UHF and fluorescence measurement techniques. (c) Variation in permittivity and tan δ of nano silica ester fluid at different temperatures be carried out through dielectric response spectroscopy. (d) Flow behavior with the viscosity variation as the function of applied shear rate and temperatures. (e) The spinning disc methodology is adopted to understand the electrostatic tendency of charge generation with the nanofluids. (f) In addition, a prediction model needs to be established to estimate static charges at higher temperatures using the electrical and rheological parameters.

II. EXPERIMENTAL STUDIES

A. SAMPLE PREPARATION

Nanofluids are prepared with natural ester Rapeseed oil (MIDEL 1204) with silica nanoparticles having an average particle size of 15 nm from Nanostructured and Amorphous Materials Inc, USA. In order to establish higher stability of nanofluid suspensions, surfactants viz. Cetyl trimethyl ammonium bromide (CTAB), span 80 and Oleic acid are applied in the present study. Moisture is eliminated from nano fillers by placing it in hot air oven at 110°C. The base fluid is mixed with the surfactant by magnetic stirring for 30 minutes and the solution is again stirred with nanoparticles inclusion. The solution is moved to probe ultrasonicator Sonic Vibra cell sonicator (500 W, 20 kHz) for a period of 3 hours at a frequency of 20 kHz. A rest period of 5 minutes is given to the nanofluid for each 30 minutes of the ultra-sonication period. Temperature of the nanofluid suspension is controlled at 40 °C with an ice bath and monitored at regular time intervals. The prepared nanofluids were placed in vacuum desiccator for the removal of micro bubbles formed during the ultra-sonication process and to avoid moisture ingression. No significant variation in colour is observed with the silica concentration and surfactants inclusions.

B. TEST CELL

High voltage is generated by using a 100 kV test transformer. A needle-plane electrode configuration is used for corona discharge and breakdown studies. The top needle electrode with a tip diameter of 5 um is in the test cell, while the plane electrode is grounded. The setup used for corona discharge and breakdown studies is carried out in a non-uniform configuration in laboratory conditions, as demonstrated in figure1.

C. SENSOR

Corona discharge is detected adopting the fluorescent fibre technique and an ultra-high frequency sensor. A non-directional UHF sensor is placed at a distance of 20 cm from the test cell. The fluorescent fiber applied for discharge detection is Saint-Gobain BCF 91A with a diameter of 1 mm. Based on the emission wavelength of the discharge activity in natural ester fluids, the green fibre is selected for corona discharge detection. The fiber core and cladding are fabricated with polystyrene and polymethyl methacrylate

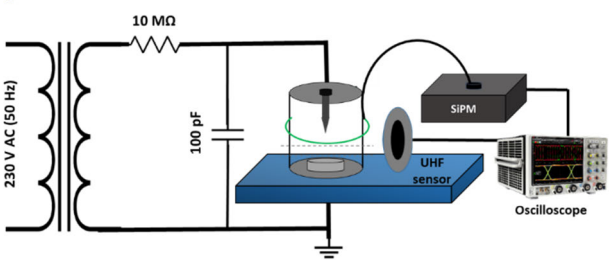

FIGURE 1. Setup used for Corona discharge and breakdown studies.

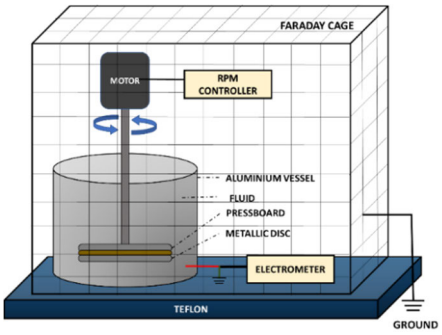

FIGURE 2. Flow electrification setup.

(PMMA) materials, respectively. Fiber is wrapped around the test cell, and its end is connected to SensL's MicroFC SMA 10050 (SiPM) module. In a transformer, the partial discharge optical spectrum lies in the range between 400 to 700 nm. The module detects light emission with a signal lasting a few nanoseconds and detects low light emissions. A DC bias voltage of 30 V is supplied to power the module. A high-frequency digital storage oscilloscope (Lecroy Model Wavepro 4 channel with 3.5 GHz bandwidth and 40 GSa/s) is used for storage and analysis of discharge signals.

D. ECT STUDIES

Fig. 2 shows the experimental setup for streaming current measurement through the spinning disc technique. The streaming current generated at the interface of the fluid with a metallic disk sandwiched cellulosic pressboard on either side. A 40 mm diameter and 6 mm thick metal disc/pressboard material is used for the study. The motor is operated to spin the disc at 600 rpm. During the test, a digital thermometer is used to monitor the temperature at different rotational speeds. To minimize the stray current interferences, the spinning disc assembly and motor were kept in a faraday cage. A Keithley 6517B pico-ammeter attached to the vessel and ground measures system charging.

Zeta potential determines the magnitude of electrostatic charges by electrochemical equilibrium at the fluid-particle interface. Measurement is carried out using Horiba SZ-100 Nano Partica instrument.

III. RESULTS AND DISCUSSION

A. ZETA POTENTIAL DISTRIBUTION WITH NANOFLUIDS

The surfactants chosen for the present study was based on their chemical structure as ionic and non-ionic surfactants to

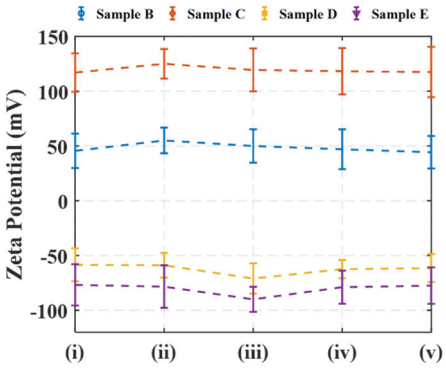

FIGURE 3. Zeta potential measurement for silica based natural ester fluid. Sample B: (i) 25 mg/L, (ii) 50 mg/L, (iii) 75 mg/L, (iv) 100 mg/L; Sample C: (i) 0.25 mg/L, (ii) 0.5 mg/L, (iii) 0.75 mg/L, (iv) 1 mg/L; Sample D: (i) 25 μl/L, (ii) 50μl/L, (iii) 75 μl/L, (iv) 100 μl/L; Sample E: (i) 25 μl/L, (ii) 50 μl/L, (iii) 75 μl/L, (iv) 100 μl/L.

estimate the adherent property with the silica nanoparticle for the nanofluid stability.

Figure 3 shows the zeta potential measurement of ester nanofluids on various concentrations of filler inclusion and surfactants. It is observed that the zeta potential increases up to a certain concentration, above which a reduction is observed due to filler agglomeration. Inclusion of surfactants alters the stability criterion by increasing the number of co-ions, resulting in an electrostatic repulsive force between fillers. However, double chain development occurs at higher concentrations of surfactant, which diminishes the electrical double layer coiling upon the particle surface, reducing its potency [14].

Silica particles are amorphous material bound with the hydroxyl group present in the ester fluid due to their weakly acidic nature. The hydrophilic surface of SiO_2 particle attain negative charge by the Silicon atom. It is observed that CTAB, as a surfactant, exhibits excellent stability in comparison to the other surfactants, oleic acid and span-80. Similar observations of zeta potential are made with the silica based synthetic ester nanofluids [15]. CTAB being cationic surfactant carries positive charged head attach itself with the hydroxyl group. The head is attached with the silica particle surface and the surfactant tail is directed onto the ester oil. This enables CTAB exhibiting good stability with a layer around the silica diminishing the effect of agglomeration. The mechanism of stabilization with oleic acid and span 80 is different from CTAB surfactants. Oleic acid is an anionic surfactant with negative head bind with the silica particle with the present of -OH group in its structure. Span 80 are non-ionic surfactants are charge less (neutral) with lipophilic head of 18 carbon atoms and the tail extends to the fluid to impart solubility to the particles. The basic difference with span-80 surfactant is the presence of 3 -OH hydrophilic group while only 1 -OH group is present in oleic acid surfactant.

The anionic and non-ionic surfactant showed negative zeta potential due to their relatively pH content dispersed in the base ester fluid. Oleic acid in the presence of unsaturated

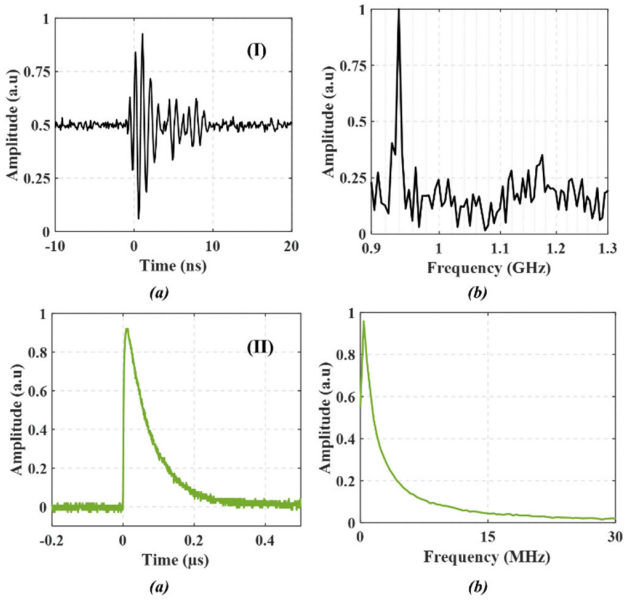

FIGURE 4. (a) Discharge signal and (b) its respective of FFT of (I) UHF and (II) Fluorescence technique.

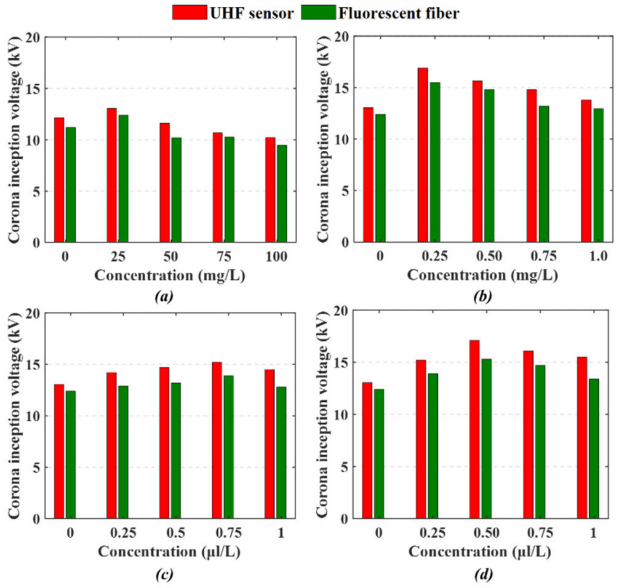

FIGURE 5. Corona inception voltage studies with different concentrations of (a) Silica, (b) Silica + CTAB, (c) Silica + Oleic acid and (d) Silica + Span-80.

hydrophobic oleyl tail of double bond alters the aggregation in the fluid. Span-80 as surfactant showed marginal increment than oleic acid which can be due to the higher number of hydroxyl groups in its structure.

B. CORONA DISCHARGE STUDIES

Corona inception voltage (CIV) is obtained with the needle plane electrode configuration. The corona discharge inception voltage obtained by adopting Ultra high frequency (UHF) and fluorescence fiber techniques. Figure 4 shows the typical UHF signal and fluorescent signal obtained due to corona discharge activity and its corresponding FFT analysis is also provided. The UHF signal acquired due to corona activity have its dominant frequency about 0.93 GHz and the fluorescence fiber output lies in the low frequency zone (few MHz to about 15 MHz) with its dominant frequency at around 1 MHz.

Figure 5 shows the experimental study of corona inception voltage with the silica based natural ester nanofluids. More than 10 measurements were carried out to arrive at the CIV and deviation in its value is less than 3%. Fluorescent fiber technique is found to be sensitive in detecting corona discharge inception in comparison to the UHF sensor technique. In addition, the energy content of the signal formed due to discharges acquired using fluorescence is higher in comparison to the UHF technique [16]. It is observed from Fig.5, the corona inception voltage increases up to certain concentrations and a decrement is observed which can be due to the act of agglomeration of particles in the fluid. The discharges are restricted by the trapping tendency of potential well around nanoparticles, reduces the fast-moving electrons slower. Considering the stability based on the CIV and zeta potential analysis, silica at 25 mg/L performed better and was chosen as the optimized concentration for surfactant inclusions. On addition of surfactants such as CTAB, span 80 and oleic acid, similar characteristics were observed with a reduction at higher loadings by the excess encapsulation of surfactant over particle surface. The optimized concentration for CTAB as surfactant is 0.25 mg/L, oleic acid is 0.75 μl/L and 0.5 μl/L for span 80. CTAB and Span 80 optimum concentrations demonstrated a 33% enhancement over the basic fluid.

The present study is mainly focused on the relevance of corona discharge studies where the stability criterion of the fluid plays a crucial role on trapping the streamer propagation by altering fast moving electrons slower. Optimization is carried based on the highest magnitude of zeta potential and the corona inception voltage at ambient temperature.

The sample code is given as silica with 25 mg/L as sample B. The optimized silica with CTAB of 0.25mg/L as Sample C, with oleic acid 0.75 μl/L as sample D and span 80 with 0.5 μl/L as sample E.

C. PARTICLE SIZE DISTRIBUTION

Figure 6 shows the particle size distribution of different silica concentrations and the inclusion of surfactants in the base fluid. The Vander walls force of attraction between the particles in the fluid is inversely proportional to the diameter of particle suspended. In order to establish higher stability of the nanofluid, a least particle size is desired. Mukherjee et al indicated a reduction in average cluster size over the ultrasonication period and relative increment in stability of the particles [17]. Higher loading of fillers reduces the inter filler distance between the particles, leading to an increase in

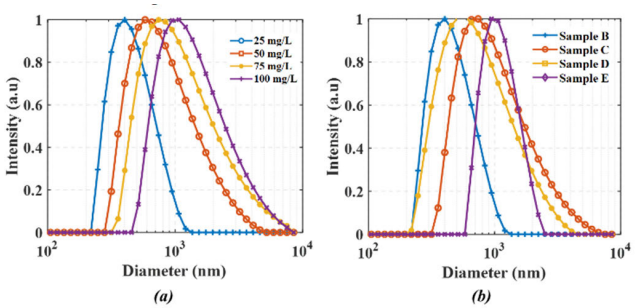

FIGURE 6. Particle size distribution of (a) Silica concentrations and (b) Nanofluids with surfactants.

TABLE 1. Dielectric parameters permittivity at 50 Hz.

Temperature	Relative permittivity (ε')		
	30°C	60°C	90°C
Sample A	3.180	3.020	2.807
Sample B	3.230	3.026	2.859
Sample C	3.261	3.050	2.831
Sample D	3.241	2.968	2.774
Sample E	3.243	3.036	2.830

their size. The mean particle size of silica at 25 mg/L shows the lowest particle diameter with better stability. Figure 6b demonstrates the particle distribution with the inclusion of surfactants. The particle exhibits a marginal increment in size with the addition of surfactants. This could be due to the encapsulation of active particle surface area, causing steric stabilization in the nanofluid. A similar observation is indicated by the increment in nanoparticle size caused by the surface coating with the oleic acid molecules [18].

D. DIELECTRIC RESPONSE SPECTROSCOPY

Dielectric response spectroscopy evaluates the relative permittivity and loss factor of the liquid in the frequency range of 0.1 Hz to 1 kHz at a voltage of 200 V. OMICRON DIRANA setup is applied for dielectric parameter as per IEC 60247 standard with the three-electrode configuration. Table 1 provides the relative permittivity at power frequency (50 Hz) under different temperatures. Weaker molecular contact and Brownian motion affect dipole orientation, reducing the dielectric constant at high temperatures [19]. Nanofluids containing insulating nanoparticle silica have a marginal increment in permittivity due to the improvement in fluid capacitance caused by nanoparticle charging. Surfactant addition increases the permittivity via enhanced interfacial polarisation at lower frequencies between the filler and the base fluid. Under the influence of the applied electric field, both the base fluid and the filler get polarized. The polarized surface charges accumulates gives the charging of particle on either sides and opposes the external electrical field.

Possible polarization occurring in a nanofluid could be due to the polarization between oil molecules, oriental polarization and inner particle polarization. Farade et al proposed a dielectric model with the influence of surfactant on Alumina (Al_2O_3) nanoparticle contribution for the oriental polarization [20].

Figure 7 shows the loss factor tan δ is measured over the frequency ranges at different temperatures of 30°C, 60°C and 90 °C. Tan delta of the nanofluids reduces with higher applied frequency due to the randomness or inability of dipole orientation on field. Also, the nanofluids exhibits higher losses in comparison to the base fluid which is due to the insufficient energy possessed by nanofluids to orient itself to the direction of electric field. The alkyl chain in ester influences the electrical conductivity of the fluid and also dependent on its viscosity. The increment in conductivity can be related to the high mobility of ions in alkyl esters [21]. Charged particles have similar motion like polar molecules with thermal random movement and orient along the direction of electric field with the oriental polarization. Sample D and E exhibits relatively lower loss factor due to the presence of hydroxyl group in its external structure. Sample C shows relatively higher permittivity and dielectric losses compared to other specimens due to its long chain molecules which requires higher energy to orient itself to the direction of electric field [22].

E. BREAKDOWN STRENGTH OF NANOFLUIDS

Figure 8 shows the breakdown strength under ac voltage profile. Nanofluids exhibits better discharge resistance to breakdown mechanism by trapping electrons in the potential distribution around the fillers which is contributed by the relaxation time of particles in the fluid. The relaxation time constant of a charged particle in the nanofluid can be given by

$$\zeta = \frac{2\varepsilon_1 + \varepsilon_2}{2\sigma_1 + \sigma_2} \tag{1}$$

where, σ_1 and σ_2 are conductivities of the ester fluid and filler respectively, ε_1 and ε_2 are the relative permittivity of the fluid and the nanoparticle respectively. The streamer propagation in a fluid can be hindered by applying nanoparticle with lower relaxation time constant which traps the electron on its surface. They are applicable only for conductive fillers, however for semi-conductive and insulative fillers the relaxation time constant is relatively higher compared to the streamer propagation. The free charges have insufficient time to accumulate on particle surface. While the streaming mechanism in this case is restricted by the charges developed by polarization altering the potential distribution on the particle surface creating potential well required for charge trapping [23]. Wang et al worked on a streamer propagation study in nanofluids based on the nanoparticle conductivity and reported the streamer velocity of fillers with variations in concentrations [24].

An enhancement of 22.8% is observed for nanofluid in the absence of surfactant in comparison to the base fluid, however the sample C in the showed up to 39.5%. The maximum breakdown strength of CTAB as surfactant inclusion is due to

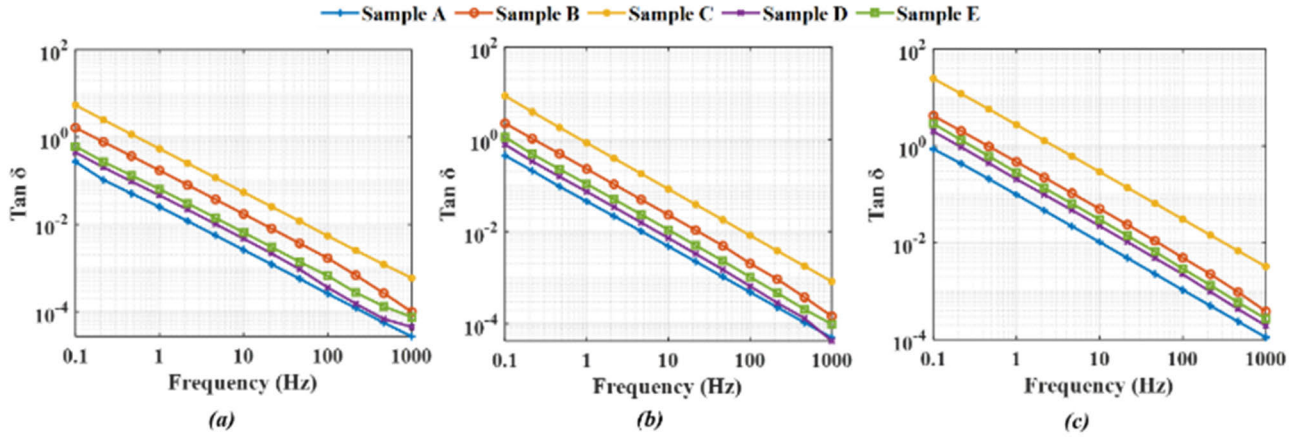

FIGURE 7. Tan delta measured at different temperature of (a) 30°C, (b) 60°C and (c) 90°C.

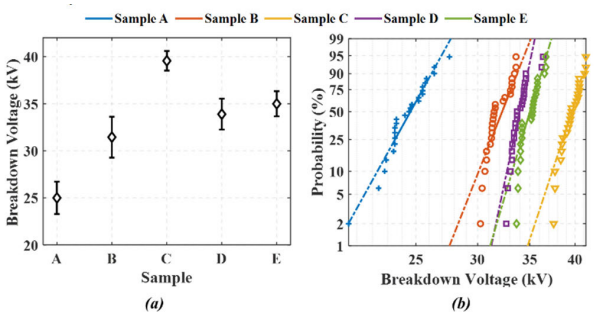

FIGURE 8. (a) Breakdown strength and (b) Weibull distribution for the ester based Nanofluids.

TABLE 2. Breakdown strength and weibull probability parameters.

Sample	Standard Deviation (σ)	Skewness	Kurtosis	Scale Parameter (η)	Shape Parameter (β)
A	1.503	-0.264	0.5629	25.091	17.74
B	1.047	0.258	-1.311	32.392	32.663
C	1.044	-0.130	-0.756	39.987	42.198
D	0.957	1.042	1.414	34.518	30.758
E	0.894	0.111	-1.059	35.453	41.807

its excellent stability. The positive head is aligned towards the filler surface and tail to the oil which makes the suspension stable to resist the streamer propagations by reducing the velocity of electrons.

1) STATISTICAL ANALYSIS OF BREAKDOWN STRENGTH

Further, the Weibull distribution is fitted for the breakdown voltage data set exhibiting a better correlation. Table 2 shows the parameters related to the breakdown strength data and fittings of Weibull distribution. Weibull distribution is denoted by

$$f\,(x, \alpha, \beta) = 1 - e^{-\left(\frac{x}{\alpha}\right)^{\beta}} \tag{2}$$

where, x is the breakdown voltage from experiment, $f(x)$ gives the probability function at breakdown, α is the scale parameter and β gives the shape parameter. Scale parameter describes the shape of compressing or stretching a data set, while shape parameter determines the slope of the probability curve. In this analysis, size and form parameters are larger, indicating less data set variability. Skewness gives the asymmetry of the probability distribution, the value in the range between -1 to $+1$ indicates a highly skewed distribution. The skewness value is positive for base fluid and nanoparticle means the breakdown data is skewed on right, samples with surfactant showed left skewness. Kurtosis determines the data set heavy or lightly tailed (outlier proneness) in relation to normal distribution providing a well fitted distribution.

F. RHEOLOGICAL ASPECTS OF SILICA BASED NANOFLUIDS

Rheological studies is carried by the cone plane geometry using the Anton paar rheometer MCR 301 in the temperature range from 30°C to 90°C. Shear strength and flow state are both influenced by the thermo-physical characteristic known as fluid viscosity, greater viscosity equals higher flow resistance.

Shear rate is applied to the natural ester and its nanofluids from 0 to 1000 s^{-1} and corresponding shear rate is measured at ambient temperature of 30°C as shown in figure 9. A linear relation is observed following the Newton's law of viscosity and are irrespective of the sample composition. Yield stress is the minimum stress applied for a material to flow. The silica based ester nanofluids initiates the stress at zero crossing referring to the null yield stress and the samples are in flow conditions. Figure 10a shows the viscosity measurement with respect to the shear rate at ambient temperature of 30°C. Due to molecular interactions in the nanofluid, the nanoparticle concentration and viscosity are directly related.

Coefficient of viscosity (μ) of a fluid is given by the $\mu = \frac{\tau}{\dot{\gamma}}$. Where, $\dot{\gamma}$ is the shear rate and τ is the shear

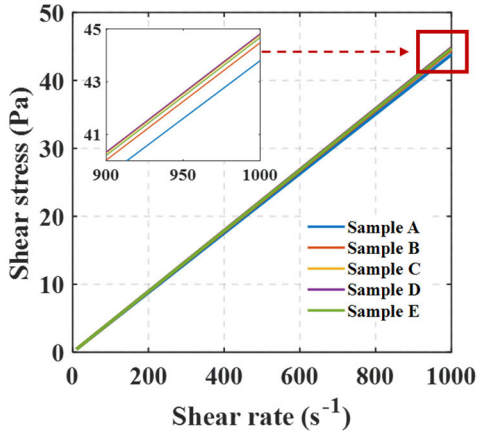

FIGURE 9. Dependency of shear stress on shear rate.

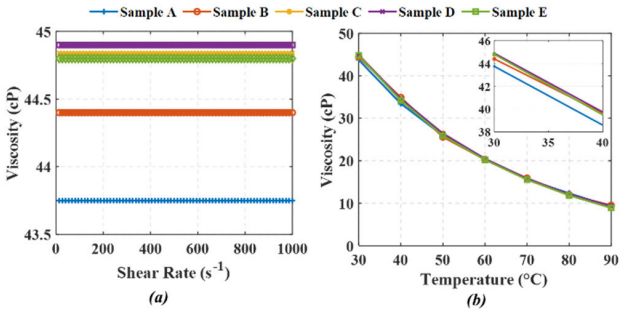

FIGURE 10. Viscosity as a function of applied (a) shear rate and (b) temperature for silica based Nanofluids.

TABLE 3. Activation energy derived from arrhenius plot.

Sample	A	B	C	D	E
Decay rate (cP/°C)	0.0106	0.0103	0.0101	0.0102	0.0101
Activation energy (kJ/mol)	23.208	23.629	24.386	23.850	24.234

stress for a Newtonian fluid. The viscosity of ester fluid and its nanofluids showed independency on the applied shear rate and exhibit a constant magnitude known as Newtonian behaviour of fluid. Least viscosity is with the base fluid followed by the sample B and followed with surfactant inclusion samples. In addition, with impact of temperature a constant shear rate of 100 s^{-1} is applied, and variation in viscosity with respective to temperature is shown in figure 10b. At lower temperatures, viscosity varies significantly, however above 55°C the nanofluid viscosity overlaps with the base fluid, exhibiting nanofluid viscosity neglect at higher temperatures. Similar observation indicated with the nanofluids for concentrating solar collectors [25]. Table 3 shows the decay rate and activation energy estimated for the plots. A minimal decrease in the viscosity degradation rate is observed with the addition of surfactants. The decaying exponential curves following

TABLE 4. Uncertainty analysis of dynamic viscosity.

Sample	Measured Viscosity (cP)		Uncertainties (%)	
	Min	Max	Min	Max
Sample A	10.05	44.60	0.038	0.045
Sample B	12.30	43.40	0.034	0.048
Sample C	9.10	44.84	0.037	0.049
Sample D	9.37	44.90	0.039	0.047
Sample E	8.90	44.80	0.037	0.043

the Arrhenius equation are controlled by the dependence of temperature on viscosity. Arrhenius equation is given by the rate constant,

$$k = A\, e^{-\left(\frac{E_a}{RT}\right)} \tag{3}$$

where, A is the frequency or pre-exponential factor, E_a is the activation energy, R is the gas constant and T is the absolute temperature. Arrhenius plot slope is used to indicate the activation energy. The required energy to dissolve the oil molecules and decrease viscosity, which reduces the mobility of the motive charge, is known as activation energy [26]. Higher activation energy is observed with the nanofluids of sample C and sample E, due to their higher stability which corresponds to higher energy to dissociate its molecule in the fluid.

Further, the uncertainty analysis is carried on the dynamic viscosity for the samples to estimate the standard deviation under different temperatures. The uncertainty of the specimen under test is determined [27],

$$\sigma = \frac{Standard\ deviation\ of\ sample\ range}{\sqrt{number\ of\ the\ sample}} \tag{4}$$

Table 4 demonstrates the uncertainty analysis of viscosity measurement for the silica based ester nanofluids fluids. The viscosity measurement is repeated 5 times for each sample at various temperatures. The standard deviation is calculated for different measurement at a distinct temperature. The uncertainties (%) of the ester based nanofluids is found to be in range of $0.34 \leq \mu > 0.049$ cP.

G. ELECTROSTATIC CHARGING TENDENCY OF NANOFLUIDS

Electrostatic charging tendency (ECT) is carried with spinning disc method to measure the current generation at the oil-pressboard interfaces. The charging characteristics depends on the flow rate, fluid and pressboard type in the system. In the present work, a comparison in current generation is estimated with the natural ester and its nanofluid as shown in tabulation V at different temperature of 30°C and 60°C. As the speed of the disc rises, the magnitude of streaming current increases. This could be due to the variability in Debye length with increasing rotational speed is possible, thereby increasing frictional strain between the disc and the insulating fluid [28]. The rate of current generation is noticed to be lower with the nanofluid inclusion of surfactants when compared

TABLE 5. Electrostatic charging tendency of nanofluids at 30° and 60°C.

Temperature	Streaming current (pA)											
	30°C						60°C					
RPM	100	200	300	400	500	600	100	200	300	400	500	600
Sample A	0.86	3.80	8.50	22.6	44.2	68.5	0.57	2.51	34.35	55.25	85.75	127.98
Sample B	0.52	11.20	15.80	19.6	20.5	36.8	0.63	4.16	32.53	38.81	72.49	92.40
Sample C	0.34	0.86	2.94	5.99	13.1	33.3	0.75	1.88	5.88	14.02	27.11	47.30
Sample D	0.55	1.56	12.70	33.2	69.1	111.02	0.88	3.01	31.35	71.75	119.65	178.14
Sample E	0.78	2	8.47	22.1	46.1	74.07	0.61	4.50	14.44	49.51	85.44	129.57

to the base fluid and silica suspended fluids. Amalanathan et al investigated the flow electrification with TiO_2 nanofillers indicating a higher generation of current magnitude in relation to the base fluids [29]. Unsaturated fatty acid content in ester oil significantly reacts with the nanoparticle molecules forming covalent bonds. Also, the viscosity increment with silica addition, alters the static charge generation in the fluid. The inclusion of surfactants in the fluid drastically suppresses the charge generation which could be due to the encapsulation mechanism of surfactants with the nanofillers. In addition, the magnitude of static charges increases with rise in temperature by the excitation of thermal ions in the fluid and also due to the viscosity reduction at higher temperatures. Surfactant inclusion sample C showed least current generation irrespective of temperature, due to its higher nanofluid stability suppressing the interaction between the fatty acids and molecules of nanoparticles.

Hotspot formation in transformer builds up the local temperature higher than usual operating temperature which alters the flow behavior of the coolant and significantly altering the charge generation and separations. A machine learning approach is adopted in the present study to estimate or predict the charging tendency at elevated temperatures.

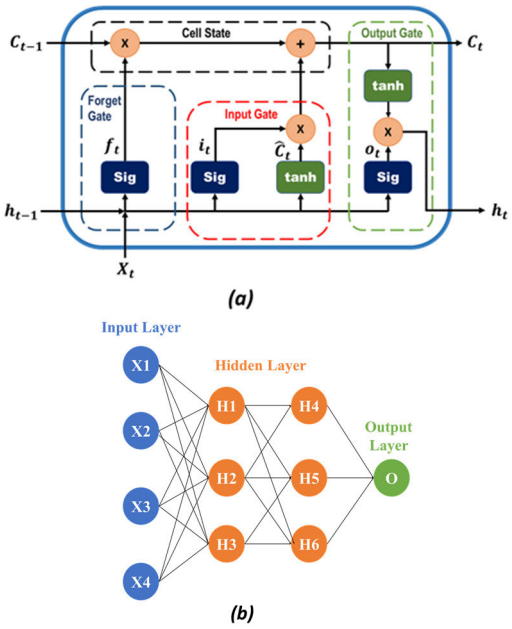

FIGURE 11. Basic architecture of (a) LSTM and (b) ANN model.

1) MACHINE LEARNING BASED PREDICTION OF ECT

The charging tendency at elevated temperature is predicted by adopting deep learning techniques, and its performance is evaluated using different error metrics. Python 3.7 and its packages like Keras, Sckit-learn, and Google TensorFlow were applied to build the Artificial Neural Network (ANN) and Long Short-Term Memory (LSTM) models.

A multi-layer-perceptron (MLP), a fully connected neural network, is employed in this work. MLP is a special kind of Artificial Neural Network (ANN) trained using the back propagation algorithm, and it is the characteristic illustration for a feed forward neural network. The sigmoid function is used for every neuron in MLP. The main advantage of the sigmoid function, which makes the training faster, is that, it takes the raw input data and transforms it to the range of 0 to 1. On completion of training, the final connection weights remain unchanged, and new input patterns are fed into the network to generate an output. Dawson et al provides further details on the back propagation learning techniques [30]. Ghoneim et al proposed a smart fault diagnostic approach for dissolved gas analysis with ANN to avoid the conflict problem for the interpretation methods [31].

Long Short-Term Memory (LSTM) is an advanced RNN based model by the remembrance of a state to make more accurate predictions. Each recurrent network is similar to a series of neural network modules that are repeated. A tanh or sigmoid function forms a typical RNN module, which is often very simple. Rediansyah et al used ANN methodology to indicate the health index of the transformer considering the quality of the oil, paper condition and Dissolved Gas Analysis (DGA). The basic issue with ANN model is the vanishing

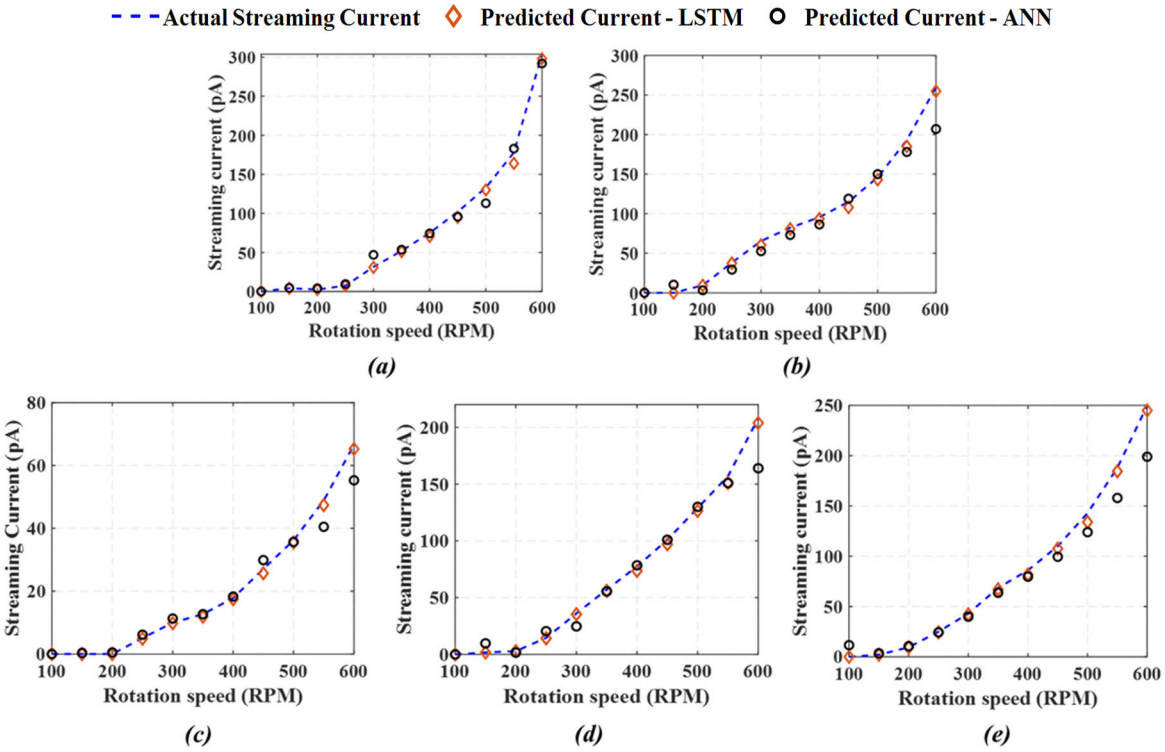

FIGURE 12. Estimation of streaming current at 90°C with LSTM and ANN models.

gradient which can be overcome by various other algorithms [32]. Zollanvari et al has utilized the LSTM model to predict various faults in the power transformer by extracting hidden patterns utilizing its vibrational signals [33]. A basic architecture of ANN and LSTM models are shown in the figure 11.

Where , X_t, h_t and C_t represents the input data, hidden state and the cell state of the LSTM model at time t. Hidden layers consisting memory cells are the major advantage of LSTM. An input layer, a hidden layer, and an output layer constitute the LSTM network model. The forget gate is responsible for eliminating the less important features from the cell state, input gate and output gate is responsible for feeding and collecting the data from the cell state. The calculation of cell state (C_t) and hidden state (h_t) are as follows,

$$C_t = f_t * C_{t-1} + i_t * \hat{C}_t \tag{5}$$

$$h_t = o_t + \tan h(C_t) \tag{6}$$

where, f_t, i_t and o_t denotes the forget gate, input gate and output gate. The forget gate (f_t) decides which data to be stored and which data to be discarded from the cell state ($\hat{C}_t$). The flow electrification parameters viz., rotation speed of the disc (RPM), temperature, viscosity of the nanofluids and conductivity are considered as the input parameters and the streaming current is set to be the target parameter. Adam optimizer is chosen with RMSE to be the loss function. For training the model, data corresponding to temperature of 30°C to 70°C is used and the streaming current at 90°C is predicted. In order to avoid over fitting, dropout layers are added and early stopping is adopted. Figure 12 shows the prediction of streaming current with the LSTM and ANN model at a temperature of 90°C.

The effectiveness and the quality of the forecast can be evaluated with several error. In this work, three error measures, namely R^2 error, root mean square error (RMSE), and mean average errors (MAE), are selected for model evaluation. RMSE are commonly used error metrics and the function indicate the average measured distance between expected and actual data points in the test set The R-Squared Error is the ratio of explained variance to total variance. Normally, the score ranges from 0 to 1. MAE is the average of the difference between the estimated current and the actual current. It is observed that the R^2 score is almost 0.99 for all the samples, inferring the effectiveness of the adopted LSTM model. Comparing the models based on RMSE and MAE metrics, it is evident that LSTM outperforms ANN in predicting the streaming current.

For comparative purposes, the model parameters, such as epochs, batch size, and learning rate, were maintained identical. Considering the computational resources as a vital issue in training the machine learning models, it can be concluded that LSTM is better than ANN for the present dataset. The major issue with ANN is that it is prone to over fit the training data. When an ANN is over trained, it learns to recognise the training patterns but finds trouble adapting to unfamiliar data [34]. Memory cells separate ANN and LSTM model frameworks, having the ability to filter

information and remember data attributes, creating a deep learning function to predict the streaming current. The ANN model has obvious disadvantages. The LSTM model is shown to be more accurate than the ANN model in these streaming current forecasts.

IV. CONCLUSION

Influence of different surfactant with ester based nanofluids on the electrical and rheological properties is the primary focus of the study. The major conclusion accrued based on the study are the following,

- Nanofluid concentrations are optimized by the zeta potential stability analysis and corona discharge studies. CTAB as surfactant (Sample C) in the base fluid exhibits maximum stability and better discharge resistance characteristics. Identification of Corona inception is sensitive adopting fluorescence fiber in comparison to the UHF technique. A maximum enhancement of about 33% is achieved in relation to the base fluid by adding Span 80 and CTAB.
- Breakdown strength of nanofluids under non-uniform electric field configuration increased drastically by altering the trap distribution of fillers. Nanofluid without surfactant improved breakdown strength of 22.8% and on CTAB surfactant inclusion showed increment up to 39.5% in comparison to the base fluid. The goodness of fit on breakdown strength data shows the failure follows Weibull distribution.
- The dielectric parameters especially the relative permittivity and loss factor significantly increases with nanofluids and is high with CTAB specimen in comparison to the anionic and non-ionic surfactants and the based fluid.
- Rheological study shows a marginal increase in viscosity with nanofluid and exhibits a constant magnitude irrespective of the applied shear rate thereby indicating Newtonian characteristics of fluid flow. Viscosity of nanofluids at transformer operating temperature shows similar characteristics as the base fluid. In addition, the activation energy obtained from the Arrhenius equation is higher with CTAB and span 80 specimens. In addition, uncertainty analysis for the viscosity for the ester based nanofluids is found to be in range of $0.34 \leq \mu > 0.049$ cP.
- The charging tendency of nanofluids drastically reduces lower than the base fluid and showed similar characteristics irrespective of the operating temperatures. Least charging tendency is observed with sample C followed with sample B, E and D.
- The Long Short-Term Memory (LSTM) and Artificial Neural Network (ANN) model are established to estimate the charging tendency at elevated hotspot temperatures. Model is trained using the dielectric and rheological parameters acquired from the current study to evaluate the working of the models. LSTM model developed in this study has reflected R^2 score equal to 0.99 almost in all the test samples. Considering other performance metrics and comparing the performance of the LSTM model with ANN model, it can be concluded that LSTM has outperformed ANN and it can be recommended for predicting the streaming current at higher temperature.

REFERENCES

[1] J. Li, R. Liao, and L. Yang, "Investigation of natural ester based liquid dielectrics and nanofluids," in *Proc. Int. Conf. High Voltage Eng. Appl.*, Sep. 2012, pp. 16–21.
[2] Y. Zhong, Y. Lv, C. Li, Y. Du, M. Chen, S. Zhang, Y. Zhou, and L. Chen, "Insulating properties and charge characteristics of natural ester fluid modified by TiO2 semiconductive nanoparticles," *IEEE Trans. Dielectr. Electr. Insul.*, vol. 20, no. 1, pp. 135–140, Feb. 2013, doi: 10.1109/TDEI.2013.6451351.
[3] J. Miao, M. Dong, M. Ren, X. Wu, L. Shen, and H. Wang, "Effect of nanoparticle polarization on relative permittivity of transformer oil-based nanofluids," *J. Appl. Phys.*, vol. 113, no. 20, 2013, Art. no. 204103, doi: 10.1063/1.4807297.
[4] Y. Lv, Y. Ge, Z. Sun, Q. Sun, M. Huang, C. Li, B. Qi, J. Yuan, and Z. Xing, "Effect of nanoparticle morphology on pre-breakdown and breakdown properties of insulating oil-based nanofluids," *Nanomaterials*, vol. 8, no. 7, p. 476, Jun. 2018, doi: 10.3390/nano8070476.
[5] S. Umar, "Investigation of the effect of pH adjustment on the stability of nanofluid," *AIP Conf. Proc.*, vol. 2031, Nov. 2018, Art. no. 020031.
[6] G. D. P. Mahidhar, R. Sarathi, N. Taylor, and H. Edin, "Study on performance of silica nanoparticle dispersed synthetic ester oil under AC and DC voltages," *IEEE Trans. Dielectr. Electr. Insul.*, vol. 25, no. 5, pp. 1958–1966, Oct. 2018, doi: 10.1109/TDEI.2018.007423.
[7] M. S. Vihacencu, P. V. Notingher, T. Paillat, and S. Jarny, "Flow electrification phenomenon for Newtonian and non-newtonian liquids: Influence of liquid conductivity, viscosity and shear stress," *IEEE Trans. Dielectr. Electr. Insul.*, vol. 21, no. 2, pp. 693–703, Apr. 2014, doi: 10.1109/TDEI.2013.004423.
[8] A. J. Amalanathan, M. Zdanowski, and R. Sarathi, "Streaming electrification of different insulating fluids in power transformers," *Energies*, vol. 15, no. 21, p. 8121, Oct. 2022, doi: 10.3390/en15218121.
[9] M. Majidi, M. S. Fadali, M. Etezadi-Amoli, and M. Oskuoee, "Partial discharge pattern recognition via sparse representation and ANN," *IEEE Trans. Dielectr. Electr. Insul.*, vol. 22, no. 2, pp. 1061–1070, Apr. 2015, doi: 10.1109/TDEI.2015.7076807.
[10] A. Kathirgamanathan, A. Patel, A. S. Khwaja, B. Venkatesh, and A. Anpalagan, "Performance comparison of single and ensemble CNN, LSTM and traditional ANN models for short-term electricity load forecasting," *J. Eng.*, vol. 2022, no. 5, pp. 550–565, May 2022, doi: 10.1049/tje2.12132.
[11] A. Y. Bhat and A. Qayoum, "Viscosity of CuO nanofluids: Experimental investigation and modelling with FFBP-ANN," *Thermochimica Acta*, vol. 714, Aug. 2022, Art. no. 179267, doi: 10.1016/j.tca.2022.179267.
[12] W. Kong, Z. Y. Dong, Y. Jia, D. J. Hill, Y. Xu, and Y. Zhang, "Short-term residential load forecasting based on LSTM recurrent neural network," *IEEE Trans. Smart Grid*, vol. 10, no. 1, pp. 841–851, Jan. 2019, doi: 10.1109/TSG.2017.2753802.
[13] Y. Shang, W. Wu, X. Huai, J. Guo, J. Su, W. Liu, Y. Huang, and L. Zhou, "Loss of life estimation of distribution transformers considering corrupted AMI data recovery and field verification," *IEEE Trans. Power Del.*, vol. 36, no. 1, pp. 180–190, Feb. 2021, doi: 10.1109/TPWRD.2020.2978809.
[14] E. G. Atiya, D.-E.-A. Mansour, R. M. Khattab, and A. M. Azmy, "Dispersion behavior and breakdown strength of transformer oil filled with TiO_2 nanoparticles," *IEEE Trans. Dielectr. Electr. Insul.*, vol. 22, no. 5, pp. 2463–2472, Oct. 2015, doi: 10.1109/TDEI.2015.004742.
[15] S. K. Amizhtan, A. J. Amalanathan, R. Sarathi, B. Srinivasan, R. L. Gardas, H. Edin, and N. Taylor, "Impact of surfactants on the electrical and rheological aspects of silica based synthetic ester nanofluids," *IEEE Access*, vol. 10, pp. 18192–18200, 2022, doi: 10.1109/ACCESS.2022.3151104.
[16] G. D. P. Mahidhar, R. Sarathi, and B. Srinivasan, "Fluorescence fiber based identification of partial discharges in liquid nitrogen for high-temperature superconducting power apparatus," *IEEE Sensors Lett.*, vol. 4, no. 2, pp. 1–4, Feb. 2020, doi: 10.1109/LSENS.2020.2971015.

[17] S. Mukherjee, P. C. Mishra, S. Chakrabarty, and P. Chaudhuri, "Effects of sonication period on colloidal stability and thermal conductivity of SiO_2-water nanofluid: An experimental investigation," *J. Cluster Sci.*, vol. 33, no. 4, pp. 1763–1771, 2021, doi: 10.1007/s10876-021-02100-w.
[18] J. Li, Z. Zhang, P. Zou, S. Grzybowski, and M. Zahn, "Preparation of a vegetable oil-based nanofluid and investigation of its breakdown and dielectric properties," *IEEE Elect. Insul. Mag.*, vol. 28, no. 5, pp. 43–50, Sep. 2012.
[19] M. H. A. Hamid, M. T. Ishak, M. F. M. Din, N. S. Suhaimi, and N. I. A. Katim, "Dielectric properties of natural ester oils used for transformer application under temperature variation," in *Proc. IEEE Int. Conf. Power Energy (PECon)*, Nov. 2016, pp. 54–57.
[20] R. A. Farade, N. I. A. Wahab, D.-E.-A. Mansour, N. B. Azis, J. B. Jasni, V. Veerasamy, A. Vinayagam, B. M. Kotiyal, and T. M. Y. Khan, "The effect of interfacial zone due to nanoparticle–surfactant interaction on dielectric properties of vegetable oil based nanofluids," *IEEE Access*, vol. 9, pp. 107033–107045, 2021, doi: 10.1109/ACCESS.2021.3098758.
[21] A. Abdelmalik, J. Fothergill, and S. Dodd, "Electrical conduction and dielectric breakdown characteristics of alkyl ester dielectric fluids obtained from palm kernel oil," *IEEE Trans. Dielectr. Electr. Insul.*, vol. 19, no. 5, pp. 1623–1632, Oct. 2012, doi: 10.1109/TDEI.2012.6311509.
[22] R. Bartnikas, *Engineering Dielectrics: Electrical Insulating Liquids*. Conshohocken, PA, USA: ASTM Monograph, 1991.
[23] T. Takada, Y. Hayase, Y. Tanaka, and T. Okamoto, "Space charge trapping in electrical potential well caused by permanent and induced dipoles for LDPE/MgO nanocomposite," *IEEE Trans. Dielectr. Electr. Insul.*, vol. 15, no. 1, pp. 152–160, Feb. 2008, doi: 10.1109/T-DEI.2008.4446746.
[24] Q. Wang, M. Rafiq, Y. Lv, C. Li, and K. Yi, "Preparation of three types of transformer oil-based nanofluids and comparative study on the effect of nanoparticle concentrations on insulating property of transformer oil," *J. Nanotechnol.*, vol. 2016, pp. 1–6, Nov. 2016, doi: 10.1155/2016/5802753.
[25] O. Gulzar, A. Qayoum, and R. Gupta, "Experimental study on stability and rheological behaviour of hybrid Al_2O_3-TiO_2 therminol-55 nanofluids for concentrating solar collectors," *Powder Technol.*, vol. 352, pp. 436–444, Jun. 2019, doi: 10.1016/j.powtec.2019.04.060.
[26] S. O. Oparanti, A. A. Khaleed, and A. A. Abdelmalik, "Nanofluid from palm kernel oil for high voltage insulation," *Mater. Chem. Phys.*, vol. 259, Feb. 2021, Art. no. 123961, doi: 10.1016/j.matchemphys.2020.123961.
[27] A. Nugroho, "Rheological characteristics and optimization of novel TiO_2-poe nanolubricant using response surface method (RSM) for air conditioning system compressor application," in *Proc. 2nd Energy Secur. Chem. Eng. Congr.*, 2022, pp. 133–146.
[28] P. Anju, B. Aryanandiny, S. K. Amizhtan, R. L. Gardas, and R. Sarathi, "Investigation on the electrical and rheological properties of AlN-based synthetic ester nanofluids," *IEEE Access*, vol. 10, pp. 37495–37505, 2022, doi: 10.1109/ACCESS.2022.3163374.
[29] A. J. Amalanathan, R. Sarathi, N. Harid, and H. Griffiths, "Investigation on flow electrification of ester-based TiO_2 nanofluids," *IEEE Trans. Dielectr. Electr. Insul.*, vol. 27, no. 5, pp. 1492–1500, Oct. 2020, doi: 10.1109/TDEI.2020.008540.
[30] C. Lv, Y. Xing, J. Zhang, X. Na, Y. Li, T. Liu, D. Cao, and F.-Y. Wang, "Levenberg–Marquardt backpropagation training of multilayer neural networks for state estimation of a safety-critical cyber-physical system," *IEEE Trans. Ind. Informat.*, vol. 14, no. 8, pp. 3436–3446, Aug. 2018, doi: 10.1109/TII.2017.2777460.
[31] S. M. S. Ghoneim, B. M. T. Ibrahim, and I. E. Nagy, "Integrated ANN-based proactive fault diagnostic scheme for power transformers using dissolved gas analysis," *IEEE Trans. Dielectr. Electr. Insul.*, vol. 23, no. 3, pp. 1838–1845, Jun. 2016, doi: 10.1109/TDEI.2016.005301.
[32] D. Rediansyah, R. A. Prasojo, and A. Abu-Siada, "Artificial intelligence-based power transformer health index for handling data uncertainty," *IEEE Access*, vol. 9, pp. 150637–150648, 2021, doi: 10.1109/ACCESS.2021.3125379.
[33] A. Zollanvari, K. Kunanbayev, S. A. Bitaghsir, and M. Bagheri, "Transformer fault prognosis using deep recurrent neural network over vibration signals," *IEEE Trans. Instrum. Meas.*, vol. 70, pp. 1–11, 2021, doi: 10.1109/TIM.2020.3026497.
[34] K. Ye, Y. Zhang, L. Yang, Y. Zhao, N. Li, and C. Xie, "Modeling convective heat transfer of supercritical carbon dioxide using an artificial neural network," *Appl. Thermal Eng.*, vol. 150, pp. 686–695, Mar. 2019, doi: 10.1016/j.applthermaleng.2018.11.031.

S. K. AMIZHTAN (Graduate Student Member, IEEE) is currently a Research Scholar with the Department of Electrical Engineering, IIT Madras, Chennai, India. His research interests include condition monitoring and characterization of nanofluid based transformer insulation.

R. AKASH is currently an Intern with the Department of Electrical Engineering, IIT Madras, Chennai, India. His research interest includes the application of machine learning in the condition monitoring of power apparatus.

RAMESH L. GARDAS is currently a Professor with the Department of Chemistry, IIT Madras, Chennai, India. His research interests include ionic liquids, chemical thermodynamics, fluid phase equilibria, group contribution methods, and structure-property correlations.

R. SARATHI (Senior Member, IEEE) is currently a Professor and the Head of the High Voltage Laboratory, Department of Electrical Engineering, IIT Madras, Chennai, India. His research interests include condition monitoring of power apparatus and nanomaterials.

B. ARYANANDINY received the M.E. degree from the Indian Institute of Science Bangalore, in 2002, and the Ph.D. degree from IIT, Chennai, in 2012. She is currently an Associate Professor with the Department of Electrical Engineering, Rajiv Gandhi Institute of Technology, Kottayam, India. She has 20 years of teaching experience. Her research interests include nanodielectrics and condition monitoring of power equipment.